Clays and Clay Minerals, Vol. 42, No. 3, 276–287, 1994.

^{27}Al MAS NMR AND ALUMINUM X-RAY ABSORPTION NEAR EDGE STRUCTURE STUDY OF IMOGOLITE AND ALLOPHANES

PH. ILDEFONSE,[1] R. J. KIRKPATRICK,[2] B. MONTEZ,[2] G. CALAS,[1]
A. M. FLANK,[3] AND P. LAGARDE[3]

[1] Laboratoire de Minéralogie-Cristallographie, UA CNRS 09,
Universités Paris 6 et 7 and IPGP, 4 place Jussieu, 75252 Paris Cedex 05

[2] Department of Geology, University of Illinois at Urbana-Champaign,
205 NHB, Urbana, Illinois 61801

[3] LURE, CNRS/CEA/MEN, 91405 Orsay

Abstract—This paper compares the results of ^{27}Al nuclear magnetic resonance spectroscopy (NMR) and Al–K-edge X-ray Absorption Near Edge Structure (XANES) of natural imogolite and allophanes and some crystalline reference minerals. All soil allophanes studied contain 4-coordinated Al (Al^{IV}). The highest relative proportion of Al^{IV}, 21% of the total Al, was found in Si-rich allophane. This value is close to that found in spring allophanes, which were previously considered to be different from soil allophanes. For a quantitative determination of the Al^{IV}/Al^{total} ratio, NMR is more reliable than XANES, because of the sensitivity of the chemical shift to low Al^{IV} concentrations, but XANES may be used even if paramagnetic impurities (mostly Fe) are present. Al–K XANES also yields more information than NMR on the local environment of Al^{VI} and especially site multiplicity. Al^{VI} XANES of imogolite and allophanes are similar regardless of the Al/Si ratio. They yield two well-resolved resonances with maxima near 1568 and 1570 eV, which indicates the presence of a unique Al^{VI} site by comparison with crystalline references. The presence of only one Al^{VI} site indicates that imogolite and allophanes have an octahedral sheet with a structure similar to 2/1 dioctahedral phyllosilicates but different from gibbsite or kaolinite, previously considered as structural analogues. The $^{27}Al^{IV}$ MAS NMR peak maxima of allophanes are between 58.6 and 59.8 ppm, in the range observed for crystalline and amorphous framework aluminosilicates, and less positive than those of sheet silicates, which are typically in the range 65–75 ppm. ^{27}Al–H^1 CPMAS NMR spectra suggest that both Al^{IV} and Al^{VI} have Al–O–H linkages.

Key Words—Allophane, Aluminum, Imogolite, NMR, XANES.

INTRODUCTION

Aluminum is an abundant element in the Earth's crust and especially in near-surface environments in which it is a major constituent of clay minerals and Al–Fe oxyhydroxides. Aluminum crystal chemistry controls the distribution of Al among the major low-temperature minerals and the stability of Al-minerals. Among the various clay minerals encountered under low-temperature conditions, aluminosilicate allophanes and imogolites are important transient phases, occurring between Al_{13} polymers and well-crystallized clay minerals. These poorly crystalline phases are common residual weathering products in soils developed on volcanic rocks, which are among the most productive soils in tropical areas (Wada, 1977; Parfitt and Henmi, 1980). They also occur in soils derived from non-volcanic crystalline and sedimentary rocks (Farmer and Russell, 1990; Parfitt, 1990; Parfitt and Kimble, 1990, and references therein) and in stream deposits (Parfitt and Henmi, 1980; Childs *et al.*, 1990). These metastable phases are highly reactive and poorly crystallized, and there is no definitive structural model for them. Allophanes constitute a chemical series from Al-rich to Si-rich compositions. Al-rich allophanes (Al/Si $\approx$ 2) are thought to have an imogolite-like structure with a gibbsitic sheet (Parfitt and Henmi, 1980). Si-rich allophanes (Al/Si $\approx$ 1) are thought to have a defect kaolin- or halloysite-structure, a tetrahedral sheet being the framework of the structure (Wada and Wada, 1977). The presence of both 4- and 6-coordinated Al in natural allophanes has been recognized by various authors (Goodman *et al.*, 1985; Childs *et al.*, 1990). However, the change in the relative concentration of Al with different coordination numbers (CN) as a function of allophane chemistry is unknown. Thus, the use of allophanes to understand the chemistry of the solutions from which they formed and the evolution of allophanes to other clay minerals is limited.

Spectroscopic methods like XANES (e.g., Brown *et al.*, 1988) and nuclear magnetic resonance (NMR) (Kirkpatrick, 1988) are direct probes of local Al-environments. ^{27}Al NMR is an important structural tool for determining Al coordination number in minerals (Müller *et al.*, 1981), particularly in clay minerals (Sanz and Serratoza, 1984; Kinsey *et al.*, 1985; Woessner, 1989) and in low temperature, XRD-amorphous aluminosilicate allophanes from soils and stream deposits (Wilson *et al.*, 1984; Goodman *et al.*, 1985; Childs *et al.*, 1990). XANES has provided useful information about Al-coordination in crystalline and glassy silicates (McKeown *et al.*, 1985; McKeown, 1989). Additional

information includes site symmetry and multiplicity and medium range structure. The sensitivity of XANES to the symmetry and number of octahedral site has been illustrated in an extensive study of crystalline model compounds with different octahedral site symmetry and with Al^{VI} site multiplicity ranging from one to four.

In this study, we present ^{27}Al MAS NMR spectra using a high spinning speed and Al–K-edge XANES of two imogolites and six allophanes with Al/Si ratios ranging from 1.1 to 2.7 and XANES spectra of some crystalline model compounds (albite, corundum, gibbsite, kaolinite, halloysite, muscovite, and pyrophyllite). The aim of this paper is to show the similarity of the local Al environment in these X-ray amorphous compounds with that found in 2/1 phyllosilicates.

EXPERIMENTAL METHODS

NMR spectroscopy

^{27}Al-NMR spectra were collected using a "home built" Fourier-transform NMR spectrometer based on an 11.7 T superconducting solenoid (130.3 MHz ^{27}Al Larmor frequency) and a Nicolet 1280 data acquisition system. A sample probe (rotor volume ≈ 0.2 ml) manufactured by Doty Scientific was used. The spectra were recorded under magic angle-spinning (MAS) conditions at spinning frequencies of 10.9–11.1 kHz. At these spinning speeds, the spinning sidebands do not overlap true peaks, and their positions are outside the range of isotropic ^{27}Al chemical shifts in aluminosilicates. The chemical shifts (reported as peak maxima, δ_p) are expressed relative to an external standard of 1 M $AlCl_3$ solution. 1300–5700 transients were collected for each spectrum. More negative peak positions (toward the right) correspond to increasing shielding and lower frequency. The accuracies of the reported δ_p vary from about 0.3–1 ppm depending of the line width observed. Short (1.6 μs) pulses and a 400 ms delay time between acquisitions were used. The relatively large H_0 field strength and the short pulses minimize loss of signal (e.g., Dupree *et al.*, 1988), but the spectra were not quantitated. Estimation of the Al^{IV}/Al^{total} ratios was made by fitting the ^{27}Al MAS NMR peak areas. Precision in fitting the spectra is better than 0.05; but as for all quadrupolar nuclides, signal can be lost due to second-order quadrupolar effects. Potential errors in the Al^{IV}/Al^{total} ratios are difficult to determine. ^{27}Al–^{1}H cross-polarization with magic angle-spinning (CPMAS) was performed on the same system by irradiating both nuclei at their respective Larmor frequencies (500 MHz ^{1}H and 130.3 MHz ^{27}Al). Hartmann-Hahn contact times (Hartmann and Hahn, 1962) ranged from 0.05 ms to 5 ms. The sample-spinning speed was 10 kHz. CPMAS enhances the signal from nuclei close to protons (e.g., Farnan *et al.*, 1987; Yang and Kirkpatrick, 1989) and is, thus, an especially useful technique for investigating OH-bearing solids.

X-ray absorption spectroscopy

Al–K XANES spectra were collected on the SA32 station at the LURE-SUPERACO synchrotron radiation facility (Orsay, France). The SUPERACO ring was operating at 800 MeV (λc = 18.6 Å) and 300 mA. The beam was monochromatized using two α-quartz crystals cut along (10$\bar{1}$0). Samples were powdered and mounted directly on copper slides after dispersion in acetone. Total electron yield spectroscopy was performed under a vacuum of 10^{-5} torr using a channeltron detector and an incidence angle between the beam and sample surface of 45°. Al–K XANES spectra were collected over a photon energy range of 1550–1600 eV, which includes the pre-edge and near-edge regions, using 0.2 eV steps. The entrance beam slits were adjusted to give a 1 eV energy resolution. All A1–K XANES spectra were calibrated with a metallic Al foil at the Al–K-edge standard photon energy value (1559 eV).

MATERIALS

We selected one natural imogolite, one synthetic imogolite, and six natural allophanes that cover the range of Al/Si ratios generally encountered in allophanes (Table 1). Al-rich allophanes with Al/Si ratios near 2 are represented by the Bealey Spur (Bs) and KiP samples that originated from podzol and dacitic weathered pumice, respectively. The highest Al/Si ratio (Al/Si = 2.7) occurs in the allophane Db from Derbyshire, which precipitated from a solution percolating from overlying weathered schist onto a limestone (MacKenzie, 1970). Si-rich allophanes with Al/Si ratios close to unity are represented by the Ok, VA, and Kk samples. Ok and VA originated from weathered andesitic ashes (Yoshinaga and Aomine, 1962; van der Gaast *et al.*, 1985), and Kk from weathered andesitic lapilli (Parfitt *et al.*, 1980). Natural imogolite KiG has been sampled with the KiP allophane (van der Gaast *et al.*, 1985). It occurs as a gel that forms thin films in dacitic pumice beds. Finally, a synthetic imogolite (Al/Si = 2) was prepared using the method of Farmer and Fraser (1979).

Crystalline model compounds for XANES include albite (Al^{IV}), α-Al_2O_3, gibbsite, poorly ordered kaolinite, halloysite and pyrophyllite (all with Al^{VI}), and muscovite (Al^{IV} + Al^{VI}). Gibbsite, kaolinite, and halloysite were chosen because they were usually considered as good structural models for allophanes (Parfitt and Henmi, 1980; Wada and Wada, 1977). The purity of these samples was checked by XRD, IR, and TEM.

RESULTS

^{27}Al MAS NMR of imogolite and allophanes

The ^{27}Al MAS NMR spectra of natural and synthetic imogolites consist of one main peak pointing at about 6.7 ppm together with spinning sidebands (ssb) (Figure 1, Table 2). A δ_p value of 6.7 ppm indicates that alu-

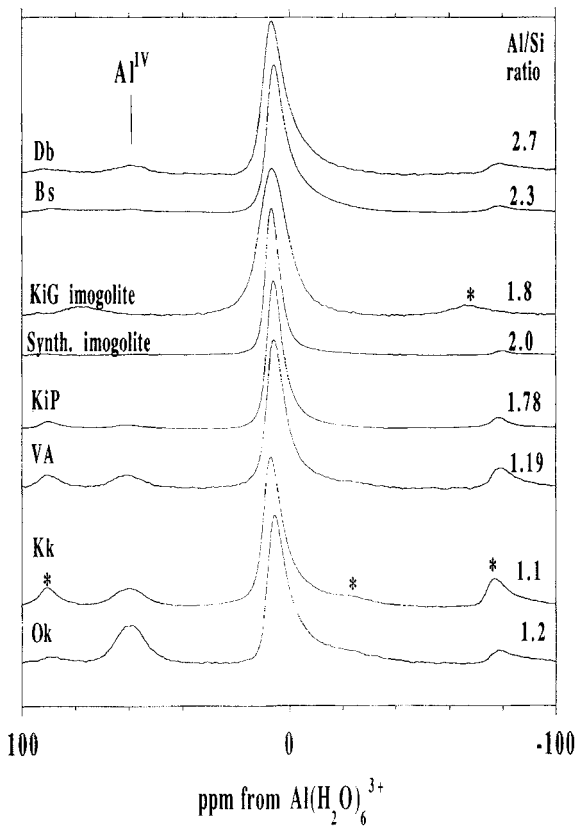

Figure 1. ^{27}Al MAS NMR spectra of imogolites and allophanes. Symbols as in Table 1. All spectra recorded at H^0 = 11.7 T and 11 kHz spinning frequency (KiG imogolite at 9 kHz). The asterisk signifies spinning sidebands.

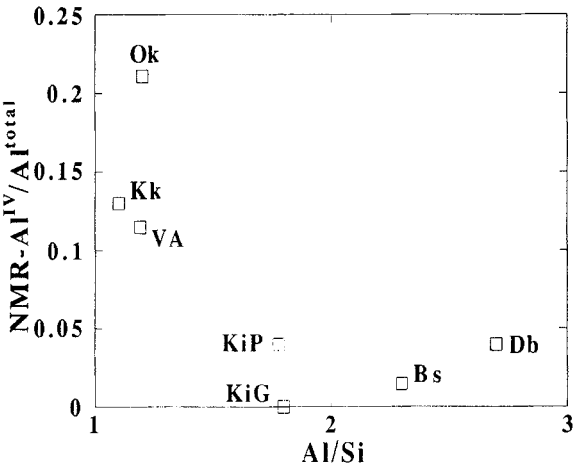

Figure 2. Relations between Al^{IV}/Al^{total} estimated from ^{27}Al MAS NMR data and Al/Si ratios of samples studied.

minum atoms are 6-coordinated (Müller *et al.*, 1981). There is no NMR peak arising from Al^{IV}. The δ_p value of the KiG imogolite is more positive than that of the same imogolite in another study (−2 ppm: MacKenzie *et al.*, 1989) due to the higher H_0 magnetic field we used (Kinsey *et al.*, 1985). It is similar to, though slightly higher than the δ_p value measured in another natural imogolite, 5.8 ppm (Goodman *et al.*, 1985). The ^{27}Al NMR spectra of Goodman *et al.* (1985) for one synthetic and one natural imogolite show, in addition to the peak for Al^{VI}, the presence of a second small peak at 63 ± 1 ppm due to Al^{IV} that was interpreted as due to the presence of an alumino silicate gel or an allophane.

There are significant differences between the ^{27}Al NMR spectra of the six allophanes studied (Figure 1, Table 2). Bs and Kip allophanes (with Al/Si ratios 2.3 and 1.78, respectively) yield spectra similar to those of imogolite, as previously observed by Goodman *et al.* (1985). The δ_p of the main resonances are 5.8 and 6.0 ppm, respectively. In addition, there are small peaks at 59.6 and 58.6 ppm due to Al^{IV} (Müller *et al.*, 1981). The spectra of the other allophanes contain peaks for both Al^{IV} and Al^{VI}. In addition, the VA and Kk allophanes yield larger spinning sidebands than the other samples, possibly due to the presence of magnetic impurities (Oldfield *et al.*, 1983; Kinsey *et al.*, 1985). In allophanes, the Al^{IV}/Al^{total} ratio determined from NMR increases with decreasing Al/Si ratio (Figure 2). It is highest for the Okamoto allophane (0.21) in which the Al/Si ratio is close to unity, as shown previously by Goodman *et al.* (1985). The Al^{IV}-δ_p values found in this study (58.6–59.8 ppm) are in the range reported for framework silicates (55–65 ppm: Fyfe *et al.*, 1982; Kirkpatrick *et al.*, 1985) and Al^{IV} in peralkaline glasses (58–62 ppm: Oestrike and Kirkpatrick, 1988). It is also

Table 1. Natural aluminosilicates gels studied and their Al/Si ratios, origin and source.

Sample	Origin	Grain size	Al/Si ratio	Reference
KiG imogolite	Kikatami, Japan	<0.2 μm	1.80	van der Gaast *et al.* (1985)
Imogolite	Synthetic		2.00	this study
Db allophane	Derbyshire, UK		2.70	MacKenzie (1970)
Bs allophane	Bealey Spur, N.Z.		2.30	Young *et al.* (1980)
KiP allophane	Iwate, Japan	<0.2 μm	1.78	van der Gaast *et al.* (1985)
Ok allophane	Okamoto, Japan		1.20	Yoshinaga and Aomine (1962)
VA allophane	Choyo, Japan	<0.2 μm	1.19	van der Gaast *et al.* (1985)
Kk allophane	Kakino, Japan	<0.4 μm	1.10	Parfitt *et al.* (1980)

https://doi.org/10.1346/CCMN.1994.0420306 Published online by Cambridge University Press

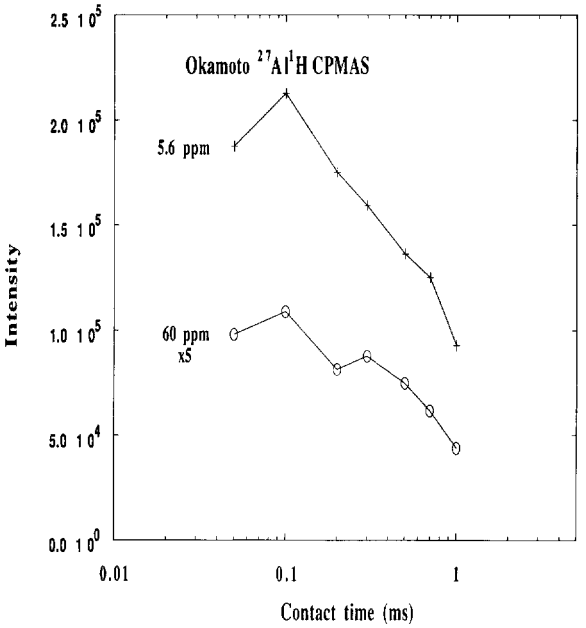

Figure 3. Intensities of Al^{IV} and Al^{VI} resonances in ^{27}Al–^{1}H CPMAS spectra with varying contact times (Okamoto allophane).

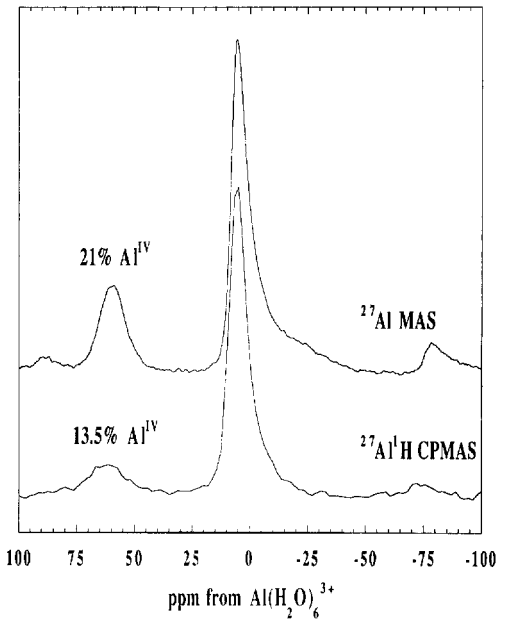

Figure 4. Comparison of 11.7 T ^{27}Al MAS and ^{27}Al–^{1}H CPMAS (contact time 0.1 ms) NMR spectra of Okamoto allophane.

close to the chemical shifts observed for the isolated tetrahedral aluminum linked to four Al octahedra in Al_{13} polymers (62 ± 1 ppm: Bottero *et al.*, 1987) and for an Al_{13} exchanged beidellite (62 ppm: Plee *et al.*, 1985). Layer silicates pillared by aluminum polyhydroxo polymers also yield Al^{IV} peak maxima of 55.7–56.3 ppm, which have been attributed to Q4(1Al) sites (Deng *et al.*, 1989). By contrast, the Al^{IV} in 2:1 phyllosilicates has δ_p values which are larger than in allophanes and imogolites (65–75 ppm: Kinsey *et al.*, 1985; Woessner, 1989).

^{27}Al–^{1}H CPMAS NMR of Okamoto allophane

The Okamoto allophane was selected for CPMAS NMR because it has the highest Al^{IV}/Al^{total} ratio, thus enabling an investigation of proton interaction with the two kinds of Al sites. Both Al^{VI} and Al^{IV} have their maximum CP intensities at a contact time of 0.1 ms (Figure 3). At this contact time, the intensity of the Al^{IV} resonance decreases relative to the MAS spectrum (Figure 4). In these conditions, the apparent Al^{IV}/Al^{total} ratio is 0.135, compared to 0.21 in the MAS experiment (Table 2). This difference indicates that the protons more efficiently cross-polarized Al^{VI} than Al^{IV}. The similarity of the contact times with maximum CP intensity for both Al^{VI} and Al^{IV} suggests the presence of Al^{IV}–O–H linkages as well as Al^{VI}–O–H linkages. The presence of Al^{IV}–O–H linkages is consistent with these sites being Bronsted acid sites (Wada, 1979) and with the pH-dependent positive and negative charges of Al^{IV}-bearing allophanes (Theng *et al.*, 1982).

Al–K-edge XANES

An Al–K X-ray absorption spectrum of kaolinite consists of two regions (Figure 5A). XANES extends within 30–50 eV above the absorption threshold. Higher photoelectron energies correspond to the domain of the Extended X-ray Absorption Fine Structure (EXAFS). XANES includes the intense sharp resonance of the absorption edge and several oscillations of lower intensity at higher energies. These absorption features arise from transitions of core electrons to the first empty electronic bound states as well as from multiple scattering resonances inside the nearest neighbor coordination shell or among the first neighbors. Because the position and relative intensity of these resonances

Table 2. ^{27}Al MAS NMR parameters and Al/Si ratios of the imogolites and allophanes studied.

Sample	Al/Si	Al^{VI} δ_p (ppm)	Al^{VI} FWHH (ppm)	Al^{IV} δ_p (ppm)	Al^{IV}/Al^{total} [1]
KiG imogolite	1.80	6.7	12.2	—	0
Synthetic imogolite	2.00	6.7	6.0	—	0
Db allophane	2.70	6.9	9.1	59.7	0.04
Bs allophane	2.30	5.8	7.7	58.6	0.015
KiP allophane	1.78	6.0	6.6	59.8	0.04
Ok allophane	1.20	5.9	8.1	58.9	0.21
VA allophane	1.19	5.9	8.0	58.9	0.11
Kk allophane	1.10	7.0	8.1	59.8	0.13

[1] Estimated from Al^{IV} and Al^{VI} peak areas.

NMR data at H_0 = 11.7 T and a MAS frequency of 11 kHz, but KiG imogolite 9 kHz.

https://doi.org/10.1346/CCMN.1994.0420306 Published online by Cambridge University Press

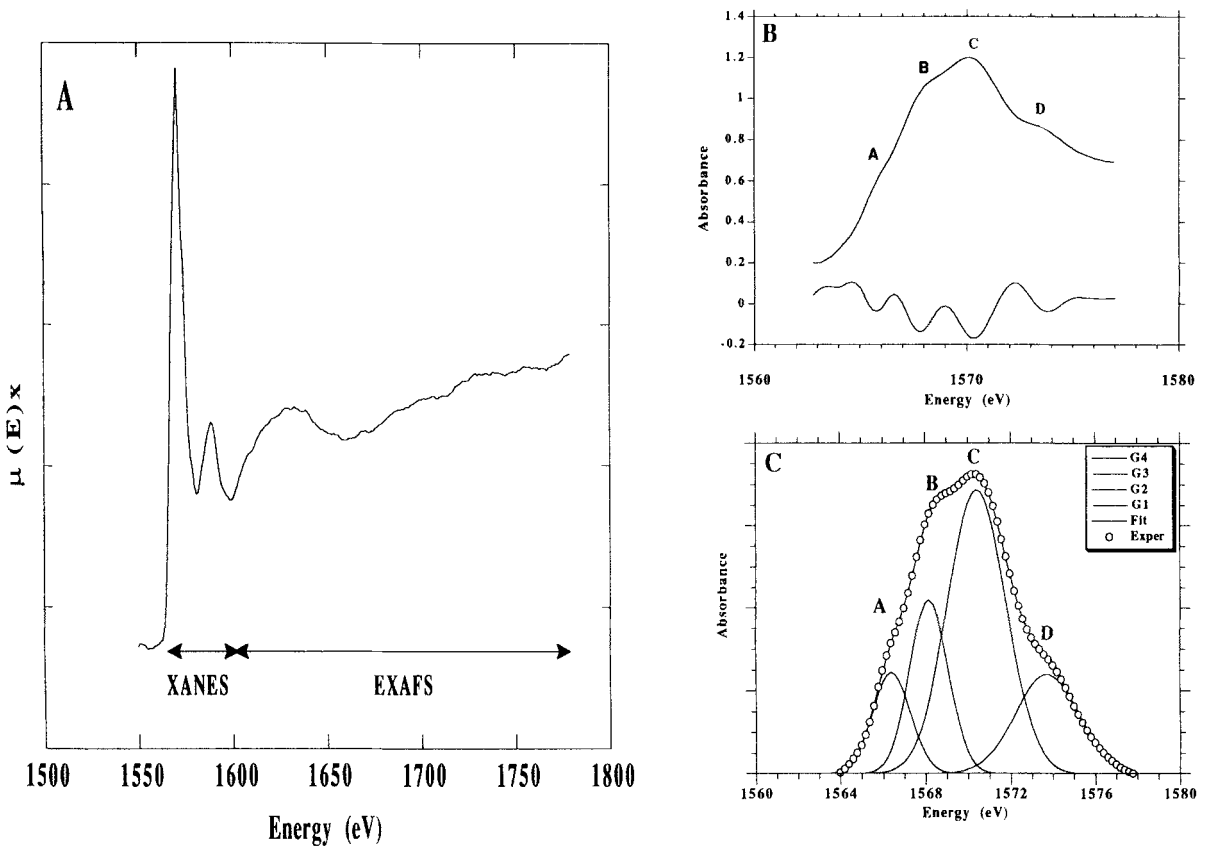

Figure 5. Example of A) Al–K XAS spectrum, B) the XANES region and its second derivative, and C) a fit by four Gaussian curves of the XANES spectrum (well-ordered kaolinite sample).

are dependent on the local structure (e.g., interatomic distances, site symmetry), it is a sensitive tool for determining the local surroundings of a given element in an unknown matrix (Petiau *et al.*, 1987; Brown *et al.*, 1988).

XANES data reduction and estimate of the Al^{IV}/Al^{total} ratio. The intensity of Al–K XANES spectra was normalized relative to the atomic absorption above the absorption threshold, extracted by a polynomial fit. They were linearly background-fitted to yield a flat pre-edge region (Figure 5B). This correction allows direct comparison with model compounds (McKeown *et al.*, 1985). The energy position of the various edge features has been determined using derivative spectra (Figure 5B). In order to estimate the relative abundance of 4- and 6-coordinated aluminum (Al^{IV} and Al^{VI}, respectively), XANES spectra were least-squares fitted using four Gaussian components, after subtraction of a polynomial background due to the atomic absorption (Figure 5C). The Gaussian shape of the components corresponds to the finite-energy resolution of the spectrometer (Lengeler and Eisenberger, 1980). At low energy, the A component corresponds to the overlap of the A feature of Al^{VI} and the Al^{IV} XANES. The other components, B, C, and D, are located at 2, 4, and 6 eV toward higher energy and are related to Al^{VI} full scattering resonances, as in Al^{VI} model compounds (see below). The average energy position and width of these components remain constant, which validates deriving the Al^{IV}/Al^{total} ratio from the ratio of the amplitude of the A component to the sum of the amplitudes of A and B components. This fitting procedure has been calibrated using a wide range of well-characterized 2/1 phyllosilicates: In smectites and illite, the Al^{IV}/Al^{total} ratios derived from the fit of the XANES spectra, using pyrophyllite as a reference ($Al^{IV}/Al^{total} = 0$), are in good agreement with those given by chemical analyses (Ildefonse *et al.*, 1992). The precision in fitting XANES spectra is 0.05. In imogolite aluminum only occurs as Al^{VI} (see above). The Al^{IV}/Al^{total} ratios of the allophanes (Table 5) were estimated relative to the imogolite spectrum (taken as a reference for Al^{VI}), and increase with decreasing Al/Si ratio. Okamoto allophane has the highest Al^{IV} content (Figure 9a).

Crystalline model compounds. The Al–K XANES spectrum of albite consists of strong single-edge maximum, A, at 1565.4 eV, which is 1.5 eV wide. At higher energy, three ill-defined, weak features (B, C, D components)

https://doi.org/10.1346/CCMN.1994.0420306 Published online by Cambridge University Press

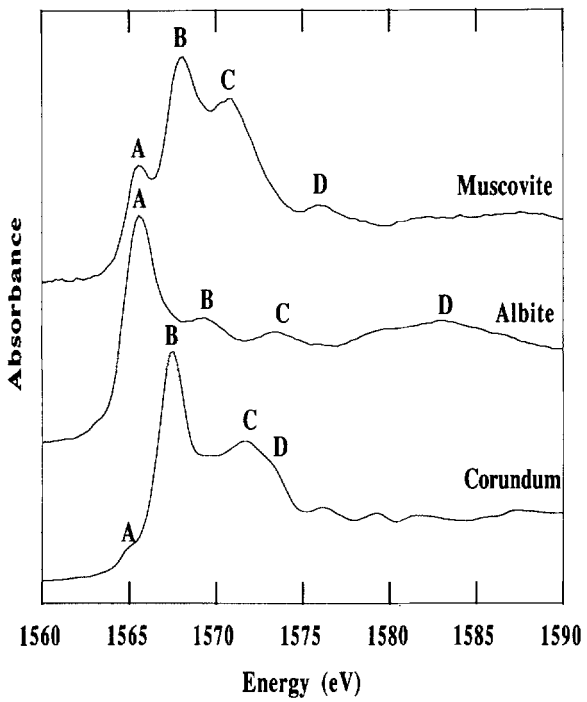

Figure 6. Al–K XANES spectra of corundum, albite, and muscovite.

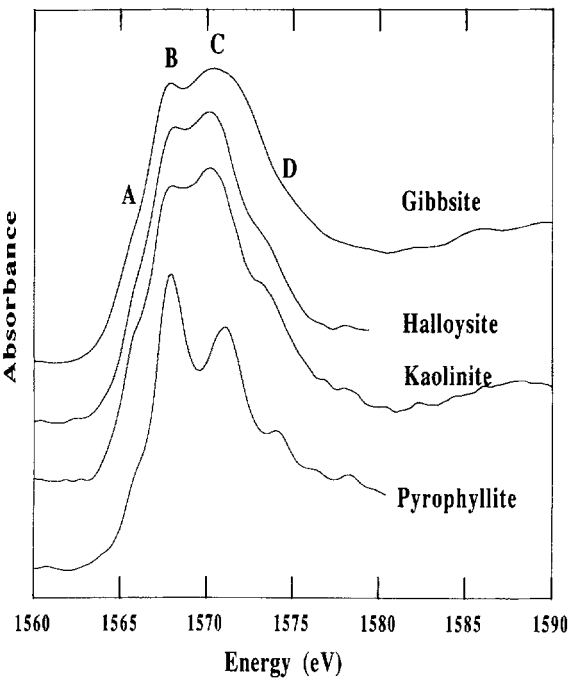

Figure 7. Al–K XANES spectra of crystalline model compounds with Al^{VI} coordinated to oxygen in a dioctahedral layer (pyrophyllite, poorly ordered kaolinite, halloysite, and gibbsite).

occur at 1569.5, 1573.5, and 1583.2 eV (Figure 6). Only small variations in the energy position and relative intensity of these various components have been observed among other Al^{IV} compounds, despite their different crystal structure and chemical composition (berlinite, natrolite, orthoclase: McKeown, 1989). The similarity of the XANES resonances in all these compounds arises from multiple scattering effects inside the coordination shell of aluminum, with only a minor contribution from the further shells.

The Al–K XANES spectrum of α-Al_2O_3 (corundum) contains four main resonances (Figure 6). The component located on the low energy side of the absorption edge (A component: 1564.7 eV) has a weak intensity. The second component, B, is the most intense and is as wide as the A component observed in the Al^{IV} XANES spectra (1.5 eV wide). It corresponds to the sharp "white line" which has been observed in Al^{VI}-bearing silicates (McKeown *et al.*, 1985). The two other features at higher energies (C and D components at 1571.6 and 1573.2 eV, respectively) are related to resonances due to single and multiple scattering from shells beyond the Al-coordination shell (McKeown, 1989). Their position, multiplicity, and relative intensity depend on the medium range structure around Al. This dependence explains the variability of Al^{VI}–K XANES spectra observed in the Al^{VI} dioctahedral reference phyllites investigated, chosen because they are built from a gibbsitic layer and all contain Al^{VI} with a 1 point symmetry. The Al–K XANES spectra contain four resonances (Figure 7), two of which remain at a constant position and weak relative intensity (A component, as a shoulder near 1565.8 eV and D component on the high energy side of the spectrum, near 1574 eV). The main difference among the XANES spectra comes from the relative intensity of the B and C resonances, although their positions show only minor variations. The intensity of C relative to B varies between 0.76 in pyrophyllite and around 1 in the other three phyllites (Table 3). The C/B intensity ratio is indeed an important parameter to characterize these XANES spectra and explains the overall shape of the XANES spectra. In pyrophyllite as in corundum, the most intense resonance corresponds to B; by contrast, the absorption maximum is shifted to the C position in the other phyllites. Finally, the Al–K XANES spectrum of gibbsite is broadened by 1 eV relative to the other spectra measured. This arises from Al–O distance distribution effects in gibbsite in which Al^{VI} occurs in two sites with six distinct Al–O distances ranging from 1.83–1.946 Å (Saalfeld and Wedde, 1974). By contrast, Al^{VI} in pyrophyllite occurs in one site with Al–O distances ranging from 1.888–1.926 Å, which may be related to the presence of two well-resolved resonances (B and C) with a maximum absorption at B. A similar situation occurs in corundum and in muscovite.

Table 3. Apparent positions in energy of main structures in Al-K XANES spectra of crystalline model compounds (positions derived from second derivative spectra) related to the point symmetry of octahedra and apparent C/B intensity ratio.

Sample	Number of Al^{VI} sites	Point symmetry	Position in energy B	Position in energy C	C/B intensity ratio
Corundum	1	3	1567.4	1571.6	0.51
Gibbsite	2	1	1567.6	1570.2	1.00
Kaolinite	2	1	1567.8	1570.6	1.04
Halloysite	2	1	1567.8	1570.8	1.01
Pyrophyllite	1	1	1567.9	1570.8	0.76
Muscovite	1	1	1567.8	1570.8	0.60

The Al–K XANES spectrum of muscovite, which contains both Al^{IV} and Al^{VI}, shows three edge maxima at 1565.4, 1567.8, and 1570.8 eV (A, B, and C, respectively: Figure 6). The A and B resonances are narrow and symmetric (2 eV wide) as C is wider (2.5 eV) and asymmetric. B has the highest amplitude and A is the least intense. By analogy with the Al–K XANES of corundum and albite and, because the spectrum of muscovite yields narrow and well-resolved resonances, feature A is related to Al^{IV} and the two resonances B and C to Al^{VI}. Al–K XANES makes a clear-cut distinction between the various Al-CNs, as previously shown in other compounds (McKeown *et al.*, 1985; McKeown, 1989), and allows estimation of the relative abundances of Al in 4- and 6-coordination.

Imogolite and allophanes. The Al–K XANES spectra of natural and synthetic imogolites and allophanes all show the presence of three main resonances, A, B and C, with a faint component D at higher energy (Figure 8). The apparent position of these components is the same at all Al/Si ratios as in Al^{VI} reference compounds (Table 4). The edge maximum corresponds to the B component, an indication of majority Al^{VI} sites, and it remains at a nearly constant position (within 0.6 eV). This edge maximum occurs at the same position as in 2:1 phyllosilicates, which contain only one type of Al^{VI} site, e.g., pyrophyllite, muscovite (Figures 6 and 7), and smectites. The C component has a lower intensity and the intensity ratio C/B remains constant at 0.80–0.84. These XANES spectra are thus different from those of other Al^{VI} model compounds such as gibbsite, halloysite, and kaolinite in which the edge maximum corresponds to the C component with a C/B ratio slightly higher than 1 (Figure 7).

Table 4. Apparent positions in energy of main structures in XANES spectra of imogolite and allophanes (positions derived from second derivative spectra) and apparent C/B intensity ratio.

Sample	A	B	C	C/B intensity ratio
KiG imogolite	1565.6	1567.7	1570.9	0.83
Db allophane	1565.6	1568.3	1570.7	0.80
Bs allophane	1565.5	1568.3	1570.6	0.80
KiP allophane	1565.4	1567.7	1570.7	0.82
Ok allophane	1565.6	1568.2	1571.0	0.84
VA allophane	1565.6	1567.7	1570.6	0.83
Kk allophane	1565.6	1568.2	1570.8	0.80

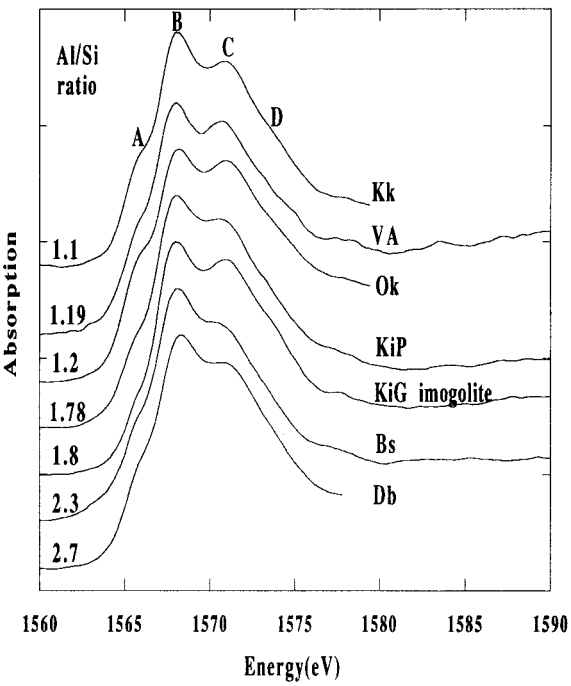

Figure 8. Al–K XANES spectra of imogolite and allophanes. Symbols as in Table 1.

Despite a similar overall shape of the spectra, XANES spectra show significant variations of the A resonance relative intensity among the samples (Table 5, Figure 9a). In natural KiG imogolite, the A feature is weak and has the same relative intensity as in all Al^{VI} reference compounds with one type of Al site. In allophanes, the increase of the relative intensity of the A shoulder indicates an increasing Al^{IV}/Al^{total} ratio with decreasing Al/Si ratio. This variation has been quantified as explained above, as the average energy position and width of the four components used in the fitting procedure show small standard deviations (Table 5). In imogolite, aluminum only occurs as Al^{VI}. This is in agreement with the structure of imogolite based on C_{2oh} symmetry (Cradwick *et al.*, 1972). In allophanes, we estimated the Al^{IV}/Al^{total} ratio (Table 5) by reference to the imogolite spectrum (Al^{IV}/Al^{total} = 0). All allophanes show the presence of Al^{IV}. The Al^{IV}/Al^{total} ratio ranges between 6.9% and 18.1% of total Al in Bealey Spur and Okamoto allophanes, respectively (Figure 9a, Table 5).

https://doi.org/10.1346/CCMN.1994.0420306 Published online by Cambridge University Press

Table 5. Results of Al-K XANES fits with four Gaussian components and estimation of Al^{IV}/Al^{total} ratios with respect to the ratio of the A/A + B amplitudes.

	KiG	Db	Bs	KiP	Ok	VA	Kk	$\bar{x}$	σn
Energy									
A	1565.5	1565.7	1565.8	1565.5	1565.7	1565.7	1565.7	1565.6	0.1
B	1567.7	1567.9	1567.9	1567.7	1567.8	1567.7	1567.8	1567.8	0.1
C	1570.8	1570.8	1570.5	1570.5	1570.8	1570.6	1570.7	1570.7	0.1
D	1574.2	1574.3	1573.9	1574.1	1574.5	1574.2	1574.2	1574.2	0.2
FWHH									
A	1.23	1.55	1.68	1.43	1.55	1.47	1.40	1.47	0.14
B	1.95	2.03	1.80	1.94	1.91	1.82	1.87	1.90	0.08
C	3.99	3.99	3.98	4.03	3.95	3.79	3.74	3.92	0.11
D	2.19	2.39	2.04	2.23	2.42	2.17	2.32	2.25	0.13
Amplitude									
C/B ratio	1.15	0.94	1.00	1.21	1.17	1.08	1.03		
A/A + B ratio	0.184	0.290	0.253	0.259	0.364	0.293	0.308		
Al^{IV}/Al^{total}	0.00	0.11	0.07	0.08	0.18	0.11	0.12		

COMPARISON OF NMR AND XANES DATA

Al coordination number

^{27}Al NMR is a sensitive method for the determination of aluminum coordination number in minerals and amorphous compounds, provided that a high magnetic field and a high spinning speed are used. In imogolite, all the aluminum is 6-coordinated to oxygen; whereas, in all allophanes studied both Al^{IV} and Al^{VI} are present, even at high Al/Si ratios. Al–K XANES is also a suitable method for the determination of CN, because the major resonances arising from Al^{IV} and Al^{VI} are separated by 2 eV. However, Al^{VI} reference compounds show a component A, located at about the same energy value as the main Al^{IV} XANES resonance. As the relative intensity of this A feature remains the same in the Al^{VI} XANES spectra of the various reference compounds investigated, it is possible to derive an Al^{IV}/Al^{total} ratio from the XANES spectra of allophanes.

The Al^{IV}/Al^{total} ratio determined in allophanes using Al–K XANES or NMR show a similar trend, i.e., an increase with decreasing Al/Si ratio (Figures 2 and 9a). Although the values derived from the two methods agree at high Al^{IV}/Al^{total} ratio, the estimates from XANES are higher than those from NMR at low Al^{IV}/Al^{total} values (Figure 9b). This discrepancy could be due to the overlap of the weak A feature of Al^{VI} XANES and of the strong A component of Al^{IV} XANES, which makes quantification difficult at low Al^{IV} contents. A preferential loss of Al^{IV} signal in NMR spectra may also be invoked (e.g., Dupree *et al.*, 1988). Because of this difficulty, NMR gives more accurate estimates of the Al^{IV}/Al^{total} ratio at low Al^{IV} contents. However, the experimental conditions used in recording the NMR spectra are important: At lower magnetic field and MAS spinning frequency than in this study, Mackenzie *et al.*, (1991) did not unequivocally determine the presence of Al^{IV} in Db, KiP and VA allophanes, due to the overlap of NMR Al^{IV} resonance with Al^{VI}-spinning sidebands.

The NMR peak maxima due to Al^{IV} (58.6–59.8 ppm) measured in our study are at a similar position as those of Q4 sites in framework silicates. This confirms the presence of highly polymerized aluminosilicate units in allophanes, in agreement with previous IR studies (Farmer and Russell, 1990). The location of Al^{IV} in allophanes must be discussed because some samples, especially the Si-rich allophanes—which have the highest Al^{IV} contents—derive from weathered volcanic glass which incorporates Al^{IV} (Oestrike *et al.*, 1987; Oestrike and Kirkpatrick, 1988; Taylor and Brown, 1979). We consider Al^{IV} as a characteristic feature of natural allophanes. Other allophanes, which do not form from weathered ashes, also contain Al^{IV} with the same NMR parameters (Derbyshire and Bealy spur allophanes in this study; synthetic gel with Al/Si = 1: Goodman *et al.*, 1985). On the other hand, Al-rich KiP and Si-rich Okamoto allophanes, though deriving from weathered volcanic materials, have a different Al^{IV} content. In addition to these considerations the Al^{IV}/Al^{total} ratio increases with decreasing Al/Si. Some of the allophanes studied here (Okamoto, Kakino, Derbyshire, Bealy Spur) have been studied previously with ^{29}Si MAS NMR (Goodman *et al.*, 1985). The ^{29}Si peak maxima near −90 ppm are not consistent with the presence of glasses with rhyolitic or dacitic composition (Oestrike *et al.*, 1987), but are more like those of less silica-rich composition (Risbud *et al.*, 1987). Similar ^{29}Si NMR spectra have been observed in stream allophanes which contain the same amount of Al^{IV} as our Si-rich samples (Childs *et al.*, 1990). However, a weak feature observed at −100 to −120 ppm in ^{29} Si NMR spectra of Derbyshire and Okamoto allophanes (Goodman *et al.*, 1985), might arise from a silica-rich glass or opal.

The ^{29}Si δ_p values found in the Si-rich allophanes

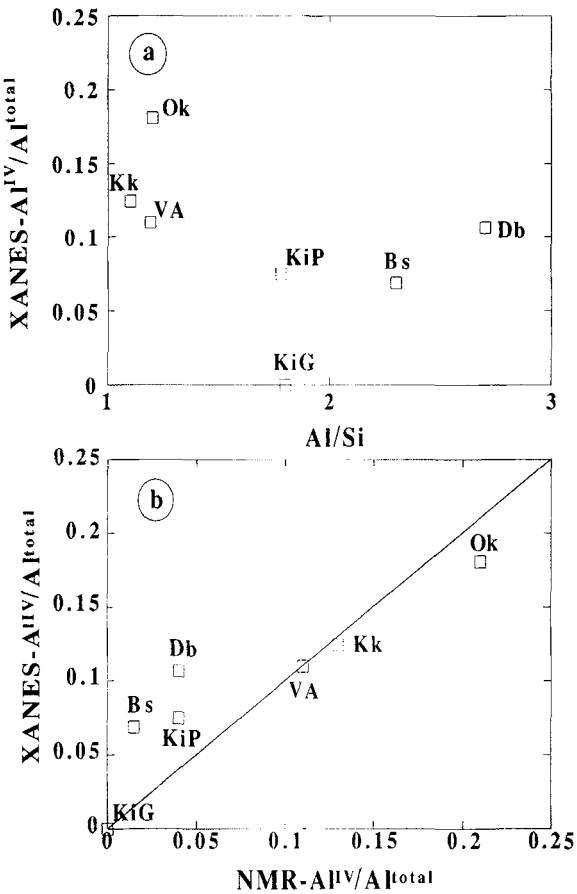

Figure 9. Relations between Al/Si ratios and Al^{IV}/Al^{total} estimated from XANES and NMR data of samples studied. a—Al/Si ratios and Al–K XANES data. b—Comparison of Al^{IV}/Al^{total} ratios measured by Al–K XANES and ^{27}Al MAS NMR.

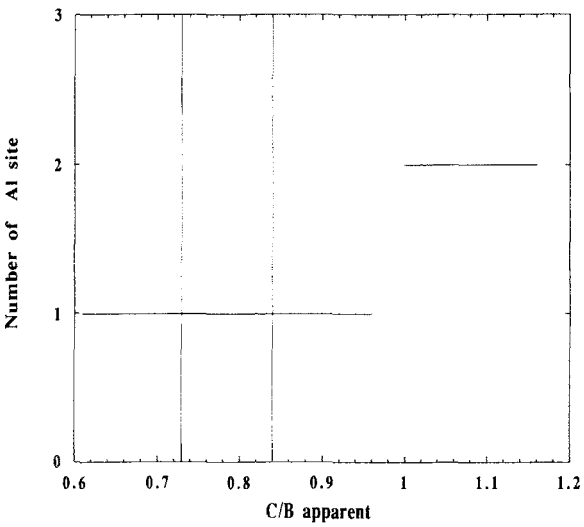

Figure 10. Range of C/B values in crystalline model compounds with one or two Al^{VI} sites (horizontal bars) and range of C/B values measured in imogolite and allophanes studied (vertical bars). C/B ratios from this study and from an upcoming Ildefonse *et al.* study.

above mentioned are similar to that of the Q3(1Al) site in muscovite. However Al^{IV} in muscovite has a δ_p of ≈72 ppm at H_0 = 11.7 T (Kinsey *et al.*, 1985) and is then less shielded than in the allophanes investigated in this study (δ_p = 58.6–59.8 ppm). δ_p allophane values are in the range of Q4 Al sites. They are also compatible with Al^{IV} having Q3 polymerization, considering that water molecules or OH groups coordinated to the Al^{IV} may cause an increased shielding or larger quadrupole coupling constant for the Al^{IV} relative to values in 2/1 phyllosilicates. Further work is needed to confirm this hypothesis.

Al^{VI} site multiplicity from XANES

Site multiplicity may be derived from Al^{VI} XANES. XANES spectra of corundum, pyrophyllite, and muscovite, which have only one Al^{VI} site, show well-resolved B and C Al^{VI} resonances, with the edge maximum at the B position (1568 eV). This confirms observations on K-alum, Al^{VI} in a single site with O_h symmetry. In gibbsite, kaolinite, and halloysite in which two distinct Al^{VI} sites exist, Al–K XANES spectra yield two poorly resolved resonances with the edge maximum at the C position (near 1570 eV). These differences may be rationalized using the results of Garcia *et al.* (1986) for octahedral aqueous complexes of transition metal cations. These authors have shown using multiple scattering calculations that the B structure is determined by a full multiple scattering resonance where all multiple scattering contributions to the total cross section are in phase. When two Al^{VI} sites are present, such as in gibbsite and kaolinite, the probability of constructive multiple scattering contributions decreases because of the distribution of site symmetry and interatomic distances. As a consequence, the amplitude of the B resonance decreases. This is experimentally confirmed by a systematic variation of the C/B ratio with site multiplicity in natural and synthetic crystalline compounds, the values of the C/B ratio distinguish minerals containing one or two Al^{IV} sites (Figure 10).We have then used the C/B value for the determination of site multiplicity in allophanes.

In the imogolite and allophanes studied, Al–K XANES spectra yield two well-resolved B and C resonances with the C resonance having the larger amplitude regardless of the Al/Si ratio. The C/B ratio is quite constant (Table 5) and occurs in the range of values determined in model compounds containing only one octahedral site (Figure 10). The local environment of Al^{VI} in imogolite and allophanes is thus close to that of compounds where Al^{VI} occurs in only one site.

An accurate description of Al site geometry using

^{27}Al NMR data is difficult because peak shape is influenced by second-order quadrupole effects, which are only partially averaged by MAS (Kirkpatrick, 1988). As far as our data are concerned, these effects are illustrated by a greater asymmetry and larger peak widths for the allophane spectra as compared to the synthetic imogolite. For the allophanes there appear to be some sites with larger quadrupole coupling constants, giving rise to the skewness to more negative peak positions. Woessner (1989) observed similar peak shapes for many clay minerals, with an Al^{VI} line broadening increasing as the Al^{IV}–Si or Al^{VI}–Mg substitution increases. Using MAS alone, however, it is not possible to separate the influence of possible ranges in chemical shift, quadrupole coupling constant, and asymmetry parameter on the ^{27}Al NMR-peak shapes in amorphous materials.

CONCLUSION

^{27}Al NMR MAS and Al–K XANES spectra show that Al is mostly 6-coordinated by oxygen in imogolites and Al-rich allophanes (imogolite-like allophane with Al/Si ratio near 2), as shown previously by ^{27}Al MAS NMR (Wilson *et al.*, 1984; Goodman *et al.*, 1985). In addition, the number and shape of the two main XANES edge maxima indicate similar Al^{VI} environments in imogolite and allophanes, regardless of their Al/Si ratios. These data agree with the model of Parfitt and Henmi (1980) in which Al-rich allophane and imogolite have close structure, the former being only more disordered at long-range distance, as the latter has a long-range structure with a repeat distance of 8.40 Å along the tube axis (Cradwick *et al.*, 1972). The Al–K XANES spectra of the imogolite and allophanes, which yield two resolved main components and a maximum position near 1568 eV, are close to those in pyrophyllite and dioctahedral smectites and suggest that Al^{VI} occupies only one octahedral site in these short-range ordered compounds. Additional data concerning the local environment around Si are needed to understand the structural changes in natural allophanes with varying Al/Si ratios. By contrast, the XANES spectra of gibbsite, kaolinite, and halloysite, minerals with two distinct Al^{VI} sites, present a broad spectrum with a maximum around 1571 eV and are then different from those of imogolite and allophanes.

All natural allophanes studied contain Al^{IV} and the Al^{IV}/Al^{total} ratio increases as Al/Si decreases. The Al^{IV}/Al^{total} value in soil allophanes with high Al/Si ratios may reach 0.21 (e.g., the Okamoto sample). This high value is of the same order as that determined in an allophane occurring as a stream deposit from Silica Spring (0.20–0.27) using ^{27}Al MAS NMR by Goodman *et al.* (1985) and Childs *et al.* (1990). In this respect, Si-rich soil allophane should not be considered different from spring allophanes. Si activity in solution thus appears to be an important parameter controlling the distribution of Al between 4- and 6-coordination. This control is emphasized when considering Al-bearing opal in which all Al is 4-coordinated to oxygen (Webb and Finlayson, 1987). In many tropical soils developed over volcanic material, halloysite and allophane coexist and it has been inferred that halloysite could be a transformation product of Si-rich gels precursors (Wada and Wada, 1977). The systematic existence of Al^{IV} in Si-rich allophanes (up to 21 percent of Al^{total} in the soil samples studied) implies a coordination change during the phase transformation. Thus, the formation of halloysite from allophane precursors can only occur by a dissolution-reprecipitation mechanism.

The availability of intense synchrotron radiation sources in the soft X-ray range opens the possibility of obtaining new information on Al and Si using X-ray absorption spectroscopy of clay minerals, poorly crystallized solid compounds (including aluminosilicates, opal-allophanes), ferrisilicates (ferrihydrite, hisingerite), and Al-substituted iron oxyhydroxides. Fe-rich materials can be studied by NMR only after chemical treatment to remove Fe-containing impurities, although such treatment may modify the structure of poorly crystalline compounds. By contrast, Al and Si–K-edge XANES may be directly recorded on natural samples, providing direct data on these reactive phases which play an important role in Al and Si surface geochemistry.

ACKNOWLEDGMENTS

We are indebted to Drs. Russell and Wada for supplying the natural samples investigated and to Dr. Herbillon for the synthetic imogolite. The Department of Geology of the University of Illinois is acknowledged for the help in the ^{27}Al MAS NMR data acquisition. The staff of LURE is acknowledged for its assistance in the XAS measurements. This study has been supported by CNRS INSU (Contribution DBT# 659 IPGP/283; Ph. I.) and NSF EAR90-04260 (R.J.K.).

REFERENCES

Bottero, J. Y., Axelos, M., Tchoubar, D., Cases, J., Fripiat, J. J., and Fiessinger, F. (1987) Mechanism of formation of aluminum trihydroxyde from Keggin Al_{13} polymers: *J. Coll. Interf. Sci.* **117,** 47–57.

Brown, G. E., Calas, G., Waychunas, G. A., and Petiau, J. (1988) X-ray absorption spectroscopy: Applications in mineralogy and geochemistry: in *Spectroscopic Methods in Mineralogy and Geology,* F. C. Hawthorne, ed., *Reviews in Mineralogy* **18,** 431–512.

Childs, C. W., Parfitt, R. L., and Newman, R. H. (1990) Structural studies of Silica Springs allophane: *Clay Miner.* **25,** 329–341.

Cradwick, P. D. G., Farmer, V. C., Russell, J. D., Masson, C. R., Wada, K., and Yoshinaga, N. (1972) Imogolite, a hydrated aluminum silicate of tubular structure: *Nature Phys. Sci.* **240,** 187–189.

Deng, Z., Lambert, J. F., and Fripiat, J. J. (1989) Pillaring puckered layer silicates: *Chem. Mat.* **1,** 640–650.

Dupree, R., Lewis, M. H., and Smith, M. E. (1988) Structural characterization of ceramic phases with high resolution ^{27}Al NMR: *J. Appl. Cryst.* **21,** 109–116.

Farmer, V. C. and Fraser, A. R. (1979) Synthetic imogolite, a tubular hydroxyaluminum silicate: in *Proc. Intern. Clay Conf., Oxford, 1978,* M. M. Mortland and V. C. Farmer, eds., Elsevier, Amsterdam, 547–553.

Farmer, V. C. and Russell, J. D. (1990) The structure and genesis of allophanes and imogolite; their distribution in non-volcanic soils: in *Soil Colloids and Their Association in Aggregates,* M. F. De Boodt, M. H. B. Hayes, and A. Herbillon, eds., Plenum Press, New York, 165–178.

Farnan, I., Kohn, S. C., and Dupree, R. (1987) A study of the structural role of water in hydrous silica glass using cross-polarization magic angle spinning NMR: *Geochim. Cosmochim. Acta* **51,** 2869–2873.

Fyfe, C. A., Gobbi, G. C., Klinowski, J., Thomas, J. M., and Ramdas, S. (1982). Resolving cristallographically distinct sites in silicalite and ZSM-5 by solid state NMR: *Nature* **296,** 530–536.

Garcia, J., Bianconi, A., Benfatto, M., and Natoli, C. R. (1986) Coordination geometry of transition metal ions in dilute solutions by XANES: *J. Phys.*, Colloque C8, **47,** 49–54.

Goodman B. A., Russell, J. D., Montez, B., Oldfield, E., and Kirkpatrick, R. J. (1985) Structural studies of imogolite and allophanes by aluminum-27 and silicon-29 nuclear magnetic resonance spectroscopy: *Phys. Chem. Minerals* **12,** 342–346.

Hartmann, S. R. and Hahn, E. L. (1962) Nuclear double resonance in the rotating frame: *Phys. Rev.* **128,** 2042–2053.

Ildefonse, Ph., Calas, G., Flank, A. M., and Lagarde, P. (1992) Local aluminum environment in clay minerals by XAS. Agronomy Abstracts, 1992 Annual Meetings, Amer. Soc. Agron., Crop Sci. Soc. Amer., Soil Sci.Soc., Clay Min. Soc., p. 373.

Kinsey, R. A., Kirkpatrick, R. J., Hower, J., Smith, K. A., and Oldfield, E. (1985) High resolution aluminum-27 and silicon-29 nuclear magnetic resonance spectroscopic study of layer silicates, including clay minerals: *Amer. Mineral.* **70,** 537–548.

Kirkpatrick, R. J. (1988) MAS NMR spectroscopy of minerals and glasses: in *Spectroscopic Methods in Mineralogy and Geology,* F. C. Hawthorne, ed., Reviews in Mineralogy **18,** 341–403.

Kirkpatrick, R. J., Smith, K. A., Schramm, S., Turner, G., and Yang, W. H. (1985) Solid-state nuclear magnetic resonance spectroscopy of minerals: *Ann. Rev. Earth Planet. Sci.* **13,** 29–47.

Lengeler, B. and Eisenberger, P. (1980) Extended X-ray absorption fine structure analysis of interatomic distances, coordination numbers, and mean relative displacements in disordered alloys: *Phys. Rev. B* **10,** 4507–4520.

MacKenzie, K. J. D., (1970) Thermal decomposition of Derbyshire allophane: *Clay Miner.* **8,** 349–351.

MacKenzie, K. J. D., Bowden, M. E., Brown, I. W. M., and Meinhold, R. H. (1989) Structure and thermal transformation of imogolite studied by ^{29}Si and ^{27}Al high-resolution solid-state nuclear magnetic resonance: *Clays & Clay Minerals* **37,** 317–324.

MacKenzie, K. J. D., Bowden, M. E., and Meinhold, R. H. (1991) The structure and thermal transformations of allophanes studied by ^{29}Si and ^{27}Al high resolution solid-state NMR: *Clays & Clay Minerals* **39,** 337–346.

McKeown, D. A. (1989) Aluminum X-ray absorption near edge spectra of some oxide minerals: Calculation *vs.* experimental data: *Phys. Chem. Miner.* **16,** 678–683.

McKeown, D. A., Waychunas, G. A. and Brown, G. E. (1985) EXAFS study of the coordination environment of aluminum in a series of silica-rich glasses and selected minerals within the Na_2O-Al_2O_3-SiO_2 system: *J. Non-Crystalline Solids* **74,** 349–371.

Müller, D., Gessner, W., Behrens, H. J., and Scheler, G. (1981) Determination of the aluminum coordination in aluminum-oxygen compounds by solid-state high resolution ^{27}Al NMR: *Chem. Phys. Letters* **79,** 59–62.

Oestrike, R. and Kirkpatrick, R. J. (1988) ^{27}Al and ^{29}Si MASS NMR spectroscopy of glasses in the system anorthite-diopside-forsterite: *Amer. Mineral.* **73,** 534–546.

Oestrike, R., Yang, W. H., Kirkpatrick, R. J., Hervig, R. L., Navrotsky, A., and Montez, B. (1987) High-resolution ^{23}NA, ^{27}Al, and ^{29}Si NMR spectroscopy of framework aluminosilicate glasses: *Geochim. Cosmoch. Acta* **51,** 2199–2209.

Oldfield, E., Kinsey, R. A., Smith, K. A., Nichols, J. A., and Kirkpatrick, R. J. (1983) High resolution NMR of inorganic solids. Influence of magnetic centres on magic angle sample-spinning lineshapes in some natural aluminosilicates: *J. Magn. Reson.* **51,** 325–329.

Parfitt, R. L. (1990) Allophane in New Zealand—A review: *Austr. J. Soil Res.* **28,** 343–360.

Parfitt, R. L. and Henmi, T. (1980) Structure of some allophanes from New-Zealand: *Clays & Clay Minerals* **28,** 285–294.

Parfitt, R. J. and Kimble, J. M. (1990) Conditions of formation of allophane in soils: *Soil Sci. Soc. Am. J.* **53,** 971–977.

Petiau, J., Calas, G., and Sainctavit, P. (1987) Recent developments in the experimental studies of XANES: *J. Phys. C9* **48,** 1085–1096.

Plee, D., Borg, F., Gatineau, L., and Fripiat, J. J. (1985) High-resolution solid-state ^{27}Al and ^{29}Si nuclear magnetic resonance study of pillared clays: *J. Am. Chem. Soc.* **107,** 2362–2369.

Risbud, S. H., Kirkpatrick, R. J., Taglialavore, A. P., and Montez, B. (1987) Solid-state NMR evidence of 4-, 5-, and 6-fold aluminum sites in roller-quenched SiO_2-Al_2O_3 glasses: *J. Amer. Ceram. Soc.* **70,** 10–12.

Saalfeld, H. and Wedde, M. (1974) Refinement of the crystal structure of gibbsite, $Al(OH)_3$: *Z. für Kristallog.* **139:** 129–135.

Sanz, J. and Serratoza, J. M. (1984) Distinction of tetrahedrally and octahedrally coordinated Al in phyllosilicates by NMR spectroscopy: *Clay Miner.* **19,** 113–115.

Taylor, M. and Brown Jr, G. E. (1979) Structure of mineral glasses: I. The feldspar glasses $NaAlSi_3O_8$, $KAlSi_3O_8$, $CaAlSi_2O_8$: *Geochim. Cosmochim. Acta* **43,** 61–75.

Theng, B. K. G., Russell, M., Churchman, G. J., and Parfitt, R. L. (1982) Surface properties of allophane, halloysite, and imogolite: *Clays & Clay Minerals* **30,** 143–149.

Van der Gaast, S. J., Wada, K., Wada, S. I., and Kakuto, Y. (1985) Small-angle X-ray powder diffraction, morphology, and structure of allophane and imogolite: *Clays & Clay Minerals,* **33,** 237–243.

Wada, K. (1977) Allophane and imogolite: in *Minerals in Solid Environments,* J. B. Dixon and S. B. Weeds, eds., Soil Science Society America, Madison, Wisconsin, 603–638.

Wada, K. (1979) Structural formulas of allophanes: in *Proc. Intern. Clay Conf., 1978, Oxford,* M. M. Mortland and V. C. Farmer, eds., *Developments in Sedimentology* **27,** Elsevier, Amsterdam, 537–545.

Wada, S. I. and Wada, K. (1977) Density and structure of allophane: *Clay Miner.* **12,** 289–298.

Webb, J. A. and Finlayson, B. L. (1987) Incorporation of Al, Mg, and water in opal A: Evidence from speleotherms: *Amer. Mineral.* **72,** 1240–1210.

Wilson, M. A., Barron, P. F., and Campbell, A. S. (1984) Detection of aluminum coordination in soils and clay frac-

tion using ^{27}Al magic angle spinning NMR: *J. Soil Sci.* **35,** 201–207.

Woessner, D. E. (1989) Characterization of clay minerals by ^{27}Al nuclear resonance spectroscopy: *Amer. Mineral.* **74,** 203–215.

Yang, W. H. and Kirkpatrick, R. J. (1989) Hydrothermal reaction of albite and a sodium aluminosilicate glass: A solid-state NMR study: *Geochim. Cosmochim. Acta* **53,** 805–819.

Yoshinaga, N. and Aomine, S. (1962) Allophane in some Ando soils: *Soil Sc. Plant. Nutr.* **8,** 6–13.

Young, A. W., Campbell, A. S., and Walker, T. W. (1980) Allophane isolated from a podzol developed on a non-vitric parent material: *Nature* **284,** 46–48.

(Received 29 March 1993; accepted 12 November 1993; Ms. 2355)